



## Feature Article

## Reprint of: Self-assembly of nanoparticles employing polymerization-induced phase separation



Roberto J.J. Williams\*, Cristina E. Hoppe, Ileana A. Zucchi, Hernán E. Romeo, Ignacio E. dell'Erba, María L. Gómez<sup>1</sup>, Julieta Puig, Agustina B. Leonardi

Institute of Materials Science and Technology (INTEMA), University of Mar del Plata and National Research Council (CONICET), Av. J. B. Justo 4302, 7600 Mar del Plata, Argentina

## ARTICLE INFO

## Article history:

Received 4 April 2014

Accepted 9 June 2014

Available online 20 June 2014

## Keywords:

Block copolymers

Nanoparticle–polymer blends

Nanoparticles

Phase separation

Polymerization-induced phase separation

Self-assembly

## ABSTRACT

Nanoparticles (NPs) may be homogeneously dispersed in the precursors of a polymer (reactive solvent) by an adequate selection of their stabilizing ligands. However, the dispersion can become metastable or unstable in the course of polymerization. If this happens, NP-rich domains can be segregated by a process called polymerization-induced phase separation (PIPS). This occurs mainly due to the decrease in the entropic contribution of the reactive solvent to the free energy of mixing (increase in its average size) and, for a reactive solvent generating a cross-linked polymer, the additional contribution of the elastic energy in the post-gel stage. The extent of PIPS will depend on the competition between phase separation and polymerization rates. It can be completely avoided, limited to a local scale or conveyed to generate different types of NPs' aggregates such as crystalline platelets, self-assembled structures with a hierarchical order and partitioning at the interface, and bidimensional patterns of NPs at the film surface. The use of a third component in the initial formulation such as a linear polymer or a block copolymer, provides the possibility of generating an internal template for the preferential location and self-assembly of phase-separated NPs. Some illustrative examples of morphologies generated by PIPS in solutions of NPs in reactive solvents, are analyzed in this feature article.

© 2015 Elsevier Inc. All rights reserved.

## Contents

1. Introduction	130
2. PIPS in binary NPs/reactive solvent formulations	130
2.1. NPs forming conventional crystals upon phase separation	130
2.2. NPs forming complex structures with a hierarchical order upon phase separation	131
2.3. Patterning of NPs in polymer films	132
2.4. Combining solvent-induced and polymerization-induced phase separation	133
2.5. Limiting PIPS to a local scale	134
2.6. Avoiding PIPS by covalently bonding the nanoparticles to the polymeric matrix	135
3. PIPS in ternary NPs/modifier/reactive solvent formulations	136
3.1. PIPS in ternary NPs/linear polymer/reactive solvent formulations	136
3.2. PIPS in ternary NPs/block copolymer (BCP)/reactive solvent formulations	136
4. Future trends	137
5. Conclusions	137
Acknowledgments	138
References	138

DOI of original article: <http://dx.doi.org/10.1016/j.jcis.2014.06.022>

\* Corresponding author. Fax: +54 2234810046.

E-mail address: [williams@fi.mdp.edu.ar](mailto:williams@fi.mdp.edu.ar) (R.J.J. Williams).

<sup>1</sup> Address: Department of Chemistry, University of Río Cuarto, 5800 Río Cuarto, Argentina.

<http://dx.doi.org/10.1016/j.jcis.2015.01.077>

0021-9797/© 2015 Elsevier Inc. All rights reserved.

## 1. Introduction

The concept of a polymerization-induced phase separation (PIPS) may be easily introduced by considering a solution of a linear polymer. The Gibbs free energy of the solution may be described by the Flory–Huggins model:

$$\Delta G/RT = (\phi_p/V_p) \ln \phi_p + (\phi_s/V_s) \ln \phi_s + (\chi/V_R)\phi_p\phi_s \quad (1)$$

In this equation  $\phi$  and  $V$  represent, respectively, volume fractions and molar volumes of polymer (P) and solvent (S),  $V_R$  is a reference volume,  $\chi$  is the interaction parameter between both components,  $T$  is the absolute temperature and  $R$  is the universal gas constant. In most cases, the interaction parameter is represented by a function of temperature and composition that takes positive values and therefore acts against the dissolution of the polymer. The first two terms are entropic contributions to the Gibbs free energy and take negative values (volume fractions are less than 1), favoring the dissolution of the polymer. However, as  $V_p \gg V_s$  the entropic contribution provided by the small solvent molecule is what permits to dissolve the polymer in the selected solvent. Besides, the chemical structure of the selected solvent must be compatible with the chemical structure of the polymer in order that the interaction parameter takes low values to make the solution possible.

In the case of a reactive solvent composed of a monomer, a hardener and catalyst or initiators, its polymerization produces a continuous increase in the average molar volume,  $V_s$ . At a certain conversion in the polymerization reaction the solution loses stability by the decrease in the absolute value of the entropic contribution to the free energy and phase separation takes place. Additionally, if a cross-linked polymer is generated, an elastic energy term must be added to the description of the Gibbs free energy in the post-gel stage [1]. This term does also contribute to the phase separation process of the linear polymer from the cross-linked polymer. But in most cases phase separation takes place before gelation driven by the increase in the average molar volume of the reactive solvent. Typical rubber-modified thermosets are obtained by this process.

PIPS also takes place when the linear polymer is replaced by other modifiers such as small organic molecules than can form a liquid crystalline phase upon phase separation. The generated dispersions of liquid crystal-rich domains in a cross-linked polymer, called polymer-dispersed liquid crystals (PDLC), are used in electro-optical devices such as reflective displays, optical switches and variable transmittance windows.

Nanoparticles (NPs) can be homogeneously dispersed in reactive solvents when the structure of chemical groups present at their surfaces is affine with the chemical structure of the solvent. The thermodynamics of these colloidal solutions can be also described by a modified Flory–Huggins equation [2]. And again, the increase in the average molar volume of the reactive solvent in the course of polymerization destabilizes the solution and might produce the phase separation and self-assembly of NPs, producing different kinds of hierarchical structures and generating specific properties in the final material (e.g., electrical conductivity generated by percolated structures of carbon nanotubes or metallic NPs). But PIPS can be avoided or limited to a local scale by covalently bonding the stabilizing ligands to the polymer matrix or by adjusting experimental conditions to generate a polymerization rate much faster than the phase separation rate.

PIPS can also take place in ternary systems including a linear or a block copolymer (BCP) in the solution of NPs in the reactive solvent. In this case, phase separated domains of the linear polymer or the BCP can act as templates for the self-assembly of NPs in the ternary blend. This can generate a variety of morphologies and structures useful for practical applications.

The aim of this feature article was to analyze a few selected examples of PIPS occurring in both binary NPs/reactive solvent formulations and ternary NPs/modifier (either a linear polymer or a BCP)/reactive solvent systems. Selected examples will illustrate the variety of organized structures that can be self-generated by NPs upon their phase separation from the solution. The article does not aim at reviewing the literature in the field but to illustrate the variety of structures and associated properties that may be generated by PIPS in solutions of NPs in reactive solvents.

## 2. PIPS in binary NPs/reactive solvent formulations

### 2.1. NPs forming conventional crystals upon phase separation

Polyhedral oligomeric silsesquioxanes (POSS) of structural formula  $(\text{RSiO}_{1.5})_n$ , where R is an organic group and  $n = 8, 10$  or  $12$ , are perfectly defined NPs with overall sizes in the range of 1 nm (depending on the size of the organic group). Typical POSS are cubes with the structure shown in Fig. 1. Due to its regular structure some POSS are crystalline with characteristic X-ray diffraction (XRD) spectra.

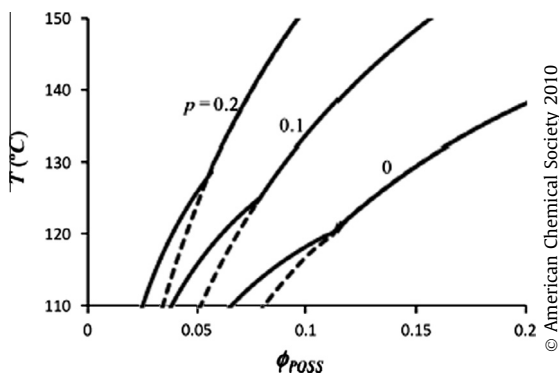
The solubility of POSS in reactive solvents can be achieved by an appropriate selection of the chemical structure of the organic groups. For example, a POSS cube with 7 isobutyl groups and 1 glycidyloxypropyl group at its corners could be dissolved at high temperatures in epoxy precursors based on stoichiometric amounts of diglycidylether of bisphenol A (DGEBA) and 4,4' methylenebis(2,6-diethylaniline) (MDEA) [3]. Fig. 2 shows the initial experimental phase diagram and the predicted phase diagrams at two advanced conversions,  $p = 0.1$  and  $0.2$ . Curves show a discontinuity at the transition from a liquid–liquid (L–L) phase separation at high temperatures to a crystal–liquid (C–L) phase separation at low temperatures. The L–L curve is continued with a dashed line in the region where the C and L are the thermodynamic stable phases. Homogeneous solutions are located at the left of the curves.

The morphologies arising from PIPS will depend on the composition of the blend and the polymerization temperature. For example, a solution with 10% by volume of POSS polymerized at  $135^\circ\text{C}$  will undergo an L–L phase separation when the conversion increases above 0.1. The final morphology is a dispersion of spherical POSS-rich domains produced by a typical nucleation-growth process (Fig. 3). Cooling from the polymerization temperature generates crystallization of POSS inside the spherical domains as revealed from XRD spectra and differential scanning calorimetry (DSC) thermograms [3].

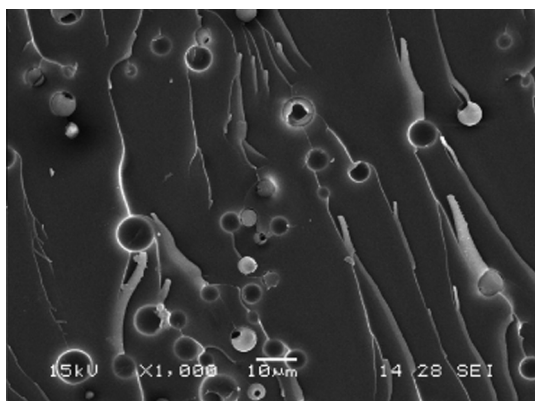
The situation changes completely if the polymerization is carried out at lower temperatures and POSS concentrations. For example, a solution with 5% by volume of POSS polymerized at  $115^\circ\text{C}$  undergoes a C–L phase separation at conversions close to 0.1. Direct crystallization generates a distribution of POSS platelets (Fig. 4). At advanced conversions the system enters the metastable L–L region and spherical domains coexisting with the crystalline platelets are also produced [3].



Fig. 1. Chemical structure of a POSS with  $n = 8$ .



**Fig. 2.** Phase diagram expressed as temperature vs. volume fraction, for a POSS cube with 7 isobutyl groups and 1 glycidyloxypropyl group at its corners dissolved in epoxy precursors based on stoichiometric amounts of diglycidylether of bisphenol A (DGEBA) and 4,4' methylenebis(2,6-diethylaniline) (MDEA), at different conversion levels,  $p = 0, 0.1$  and  $0.2$ . Reproduced with permission from Di Luca et al. [3].



**Fig. 3.** SEM micrograph of the dispersion of POSS-rich domains in the epoxy matrix for a polymerization carried out at 135 °C. Reproduced with permission from Di Luca et al. [3].

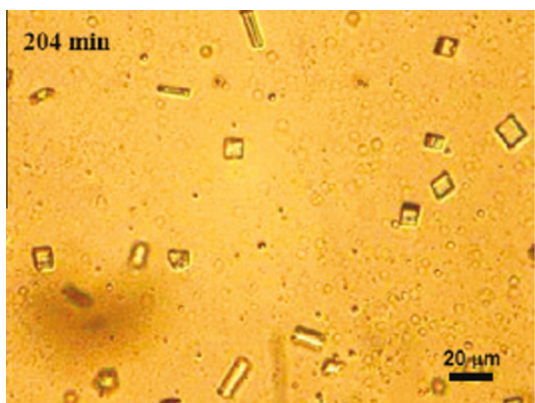


**Fig. 4.** Optical micrograph of the dispersion of POSS crystalline platelets dispersed in the epoxy matrix for a polymerization carried out at 115 °C. Reproduced with permission from Di Luca et al. [3].

The generation of crystalline platelets in a cross-linked polymer by PIPS, can mimic some of the properties of thermosets modified by exfoliated nanoclays (decrease in the permeability to gases and increase in mechanical and thermal properties). The significant advantage is the ease of processing because POSS cubes generate crystalline platelets *in situ* and therefore, there is no need to care

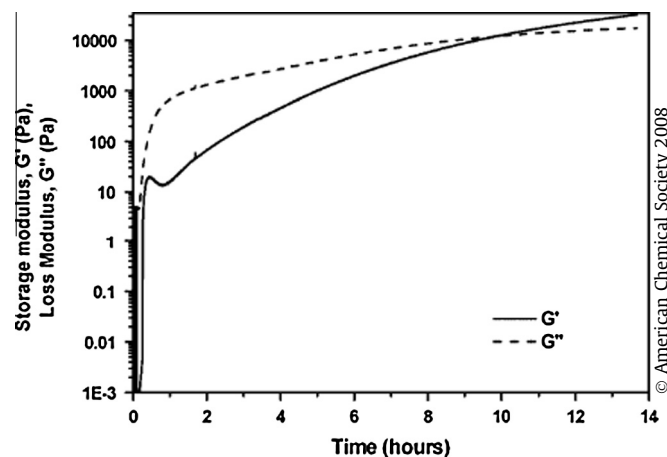


**Fig. 5.** Evolution of the storage and loss modulus of a solution of stoichiometric amounts of DGEBA and DA containing 0.15 wt% gold NPs stabilized by dodecyl chains, during polymerization at 100 °C. Reproduced with permission from Zucchi et al. [5].

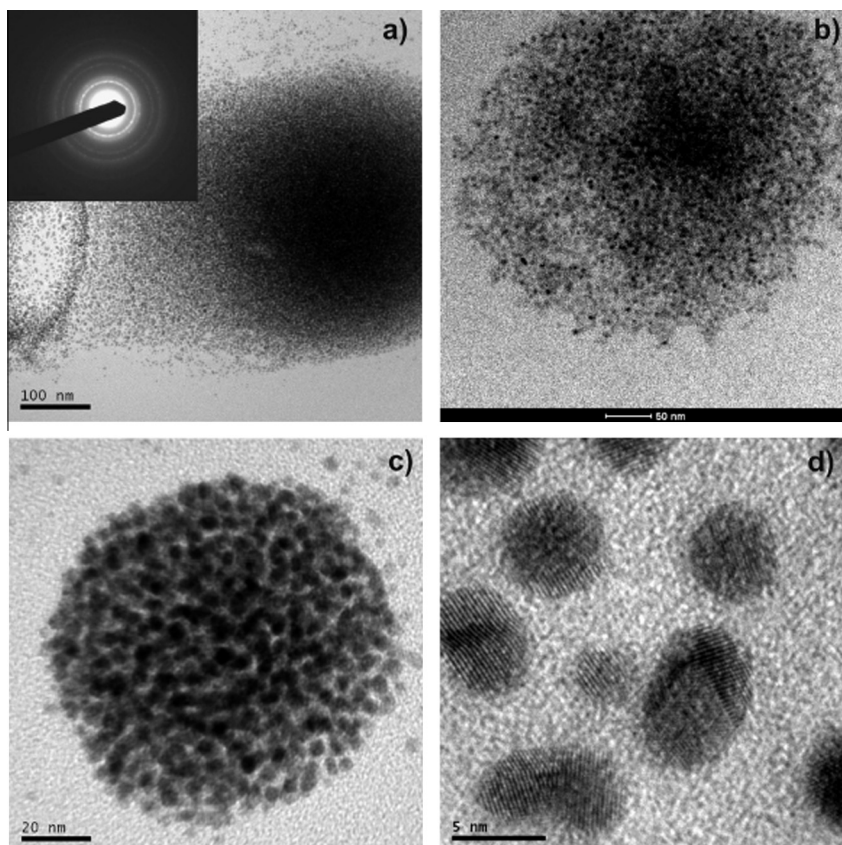
about clay exfoliation or the transport of highly-viscous solid-liquid dispersions. The practical application of this concept would require a POSS-reactive solvent solution with a phase diagram showing only a C-L equilibrium and no possibility of L-L phase separation.

## 2.2. NPs forming complex structures with a hierarchical order upon phase separation

NPs can be synthesized with different shapes, sizes and organic groups attached at their surfaces. These organic groups can be covalently or physically bonded and their chemical nature drives their solubility in a reactive solvent. As an example, gold NPs stabilized by dodecyl chains (arising from dodecanethiol molecules bonded to the gold surface through the S atom), can be synthesized by conventional methods. The typical Brust-Schiffrin process [4], leads to gold NPs with an average size close to 2 nm that are stabilized with dodecyl chains. These NPs could be dissolved in epoxy precursors based on stoichiometric amounts of DGEBA and dodecylamine (DA) [5]. The solubility arises from the matching of the chemical structures of DA and the organic groups attached to the NPs. The reaction of DGEBA and DA leads to a linear polymer that generates a physically cross-linked gel by tail-to-tail association of the dodecyl groups of DA [5].

PIPS takes place in a solution containing 0.15 wt% gold NPs in stoichiometric amounts of DGEBA and DA, polymerized at 100 °C. Fig. 5 shows the evolution of the loss and the storage modulus along the reaction. The cross-over of both moduli is characteristic of the formation of a physical gel by the tail-to-tail association of dodecyl chains. The intermediate decrease in the storage modulus was related to the phase separation of gold NPs during polymerization, a fact that produced a partial disruption in the association of dodecyl chains. The intermediate decrease in the storage modulus was not observed for the polymerization of the neat matrix.

Fig. 6(a–c) shows representative transmission electron microscopy (TEM) images of colloidal crystals constituted by gold NPs trapped in the epoxy matrix. The inset in (a) shows the selected-area electron diffraction (SAED) pattern of gold NPs. The diffraction ring pattern is characteristic of polycrystalline gold. The high-resolution TEM (HRTEM) image (Fig. 6d) shows the presence of crystalline gold planes in individual nanocrystals. But the most striking feature is the increase in the size of individual nanocrystals, from about 2 nm in the initial population to about 5 nm in



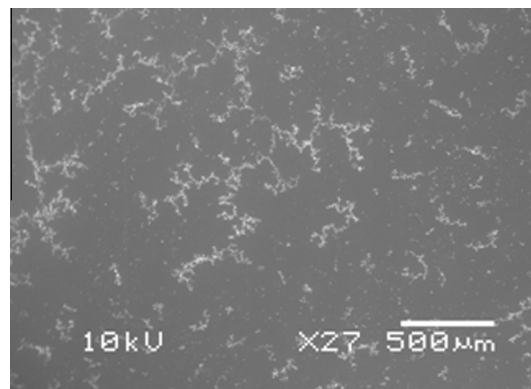
© American Chemical Society 2008

**Fig. 6.** (a–c) Representative TEM images of colloidal crystals constituted by gold NPs trapped in the epoxy matrix, and (d) HRTEM image showing the presence of crystalline planes in individual nanocrystals. The inset in (a) shows the SAED pattern of gold NPs. The diffraction ring pattern is characteristic of polycrystalline gold. Reproduced with permission from Zucchi et al. [5].

the final distribution, a size that was not present in the initial distribution. This means that the first process that took place after phase separation was the coalescence of gold NPs leading to a narrower size distribution than the initial one. In fact, a strategy to obtain narrow distributions of small gold NPs stabilized by alkanethiol chains is to heat them in a concentrated solution [6,7]. This produces the partial desorption of dodecanethiol moieties followed by aggregation and coalescence of nude gold NPs and re-adsorption of the stabilizing organic chains. This process can be employed to increase the average size of gold NPs from about 2 nm to 5.2 nm [6]. This same process took place spontaneously in the reacting system during phase separation at 100 °C.

As shown in Fig. 6(a–c), the 5-nm gold NPs self-assembled into colloidal crystals with sizes in the range of tens to hundreds of nanometers. Small angle X-ray scattering (SAXS) spectra showed a 3D hexagonal closed-packed (HCP) array of gold NPs. The characteristic size of the core of gold NPs obtained from the HCP array was 5 nm, in agreement with the size observed in TEM images. Then, there are two levels of crystalline organization: the one of gold atoms inside individual NPs and the one of NPs in the colloidal crystal.

Partitioning and irreversible adsorption of large colloidal crystals at the air–epoxy interface is expected due to the high energy (relative to thermal energy) that is necessary to remove the particles from the surface [8]. Scanning electron microscopy (SEM) images of the air–epoxy interface show large aggregates of colloidal crystals (Fig. 7). Irreversible diffusion-limited-aggregation models account for the formation of these highly ramified fractal structures [9–11]. Most of the gold NPs dispersed in the epoxy precursors ended in these aggregates present at the interface of



© American Chemical Society 2008

**Fig. 7.** SEM image showing large aggregates of colloidal crystals of gold NPs at the air–epoxy interface. Reproduced with permission from Zucchi et al. [5].

the sample. By adjusting the thickness of the sample and the amount of gold NPs in the initial formulation, a percolating structure of colloidal crystals might be generated by PIPS. By decreasing the size of the alkyl group that stabilizes individual NPs, the superficial electrical conductivity might reach adequate values for the use of these materials as antistatic coatings.

### 2.3. Patterning of NPs in polymer films

Photoluminescent NPs or nanorods may be patterned in polymer films by combining lithographic techniques with PIPS

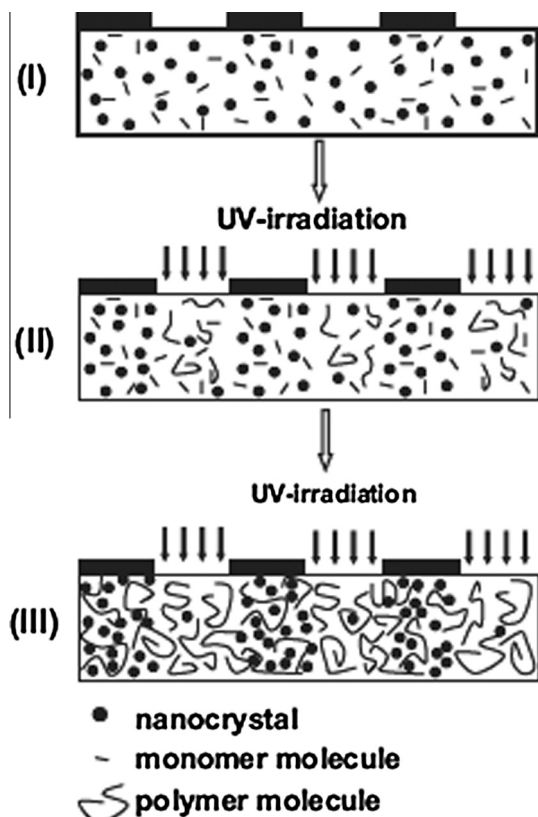


**Fig. 8.** Schematic of lithographic PIPS. I. A homogeneous mixture of monomer, photoluminescent NPs and photoinitiator before polymerization; II. The material is UV-irradiated through a shadow mask; NPs are phase-separated by PIPS and concentrate in the regions protected by the mask; III. End of polymerization in both regions. Reproduced with permission from Paquet et al. [12].

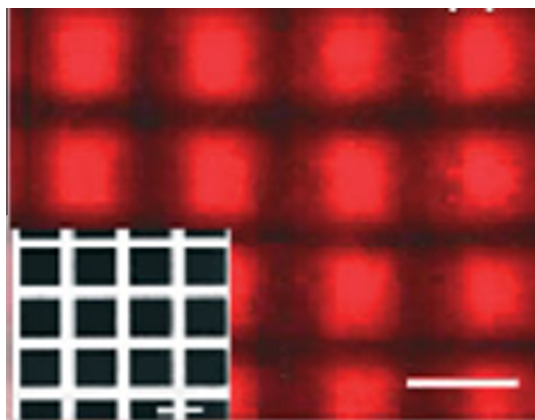


**Fig. 9.** Regular pattern generated from a 2 wt% solution of photoluminescent CdSe–ZnS core-shell NPs stabilized with trioctyl phosphine oxide in 2-ethylhexyl methacrylate, in the presence of hydroxycyclohexyl phenyl ketone as photoinitiator. The optical micrograph of the shadow mask is shown in the inset. The scale bar is 400  $\mu\text{m}$ . Reproduced with permission from Paquet et al. [12].

[12,13]. Production of pre-designed bidimensional patterns of photoluminescent regions is an important requirement for various photonic, biomedical and optoelectronic applications. Fig. 8 illustrates this approach starting from a homogeneous dispersion of NPs in a monomer in the presence of a photoinitiator. UV-irradiation through a shadow mask produces the polymerization and the phase separation of NPs by PIPS. NPs diffuse and concentrate in the monomer-rich areas where they are still soluble. In this way,

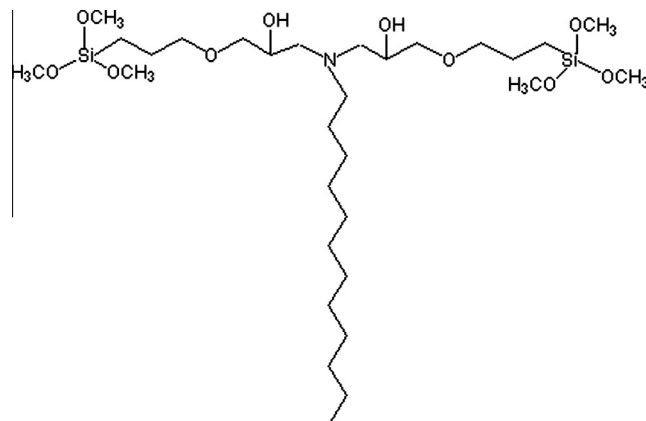


**Fig. 10.** Chemical structure of a monomer containing a dodecyl chain and six polymerizable methoxysilane groups.

the areas protected from irradiation become enriched in NPs while the irradiated regions become deficient in NPs. Eventually, polymerization takes place in the areas protected by the mask, initiated by the diffusion of species containing radicals to the regions under the mask. The polymerized film forms a negative patterned replica of the shadow mask.

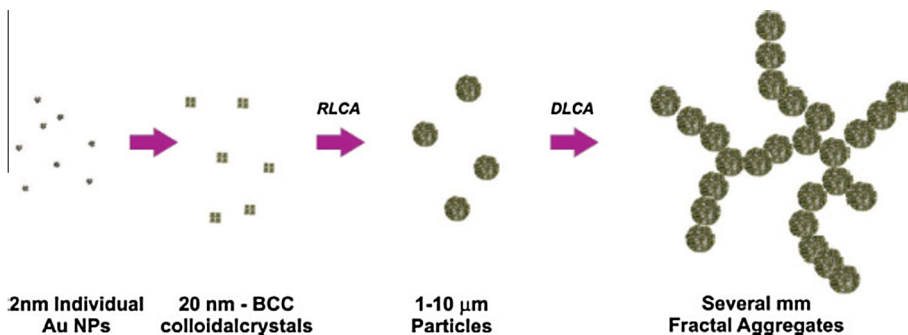
Fig. 9 is a confocal fluorescence microscopy image showing a regular photoluminescent pattern generated from a 2 wt% solution of CdSe–ZnS core-shell NPs stabilized with trioctyl phosphine oxide in 2-ethylhexyl methacrylate, in the presence of hydroxycyclohexyl phenyl ketone as photoinitiator [12]. In order to generate regular patterns it was necessary to match the cloud point (start of PIPS) with the increasing viscosity of the polymerizing system, to use a film thickness less than 200  $\mu\text{m}$  to suppress natural convection patterns, and to select a convenient feature size of the mask [12]. When NPs were replaced by nanorods, the lateral diffusion produced an alignment of nanorods in the regions located under the mask [13].

#### 2.4. Combining solvent-induced and polymerization-induced phase separation

The hydrolysis and condensation of monomers functionalized with alkoxy silane groups (sol–gel reactions) is normally produced in the presence of a solvent that is slowly evaporated in the course of polymerization. If NPs stabilized with suitable organic ligands are incorporated into these formulations, a complex phase separation process can take place induced by both solvent evaporation and polymerization.

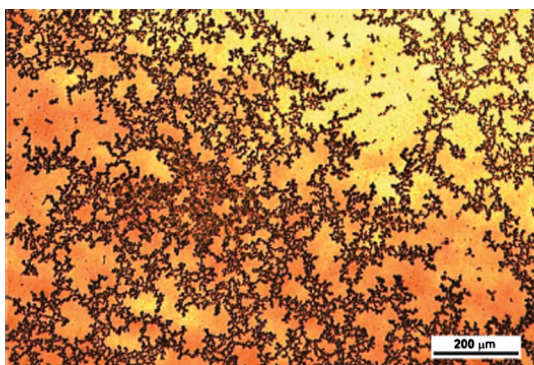
The multifunctional monomer shown in Fig. 10 containing a pendant dodecyl chain was mixed with up to 1 wt% of 2-nm gold NPs stabilized with dodecyl groups and the blend was dissolved in tetrahydrofuran (THF). A 0.1 M solution was polymerized at 18 °C by adding suitable amounts of formic acid (molar ratio HCOOH/Si = 0.1) and water (molar ratio H<sub>2</sub>O/Si = 3) [14]. The reaction took place during several weeks with a slow solvent evaporation. Free-standing films were obtained after this period.

A detailed characterization of the final structure revealed that phase separation and self-assembly of gold NPs followed a multi-step process [14]. Small body-centered cubic (bcc) colloidal crystals of about 20 nm diameter were formed in a first step by aggregation of the 2-nm NPs present in the initial formulation. Then, a reaction-limited colloid aggregation (RLCA) process [9] of the small colloidal crystals generated micrometer-sized spherical particles that formed fractal structures at the air–polymer interface by a diffusion-limited colloid aggregation (DLCA) process. Fig. 11



© American Chemical Society 2009

**Fig. 11.** Self-assembly of 2-nm gold NPs induced by simultaneous solvent evaporation and sol-gel polymerization of a multifunctional monomer at room temperature. Reproduced with permission from Gómez et al. [14].



© American Chemical Society 2009

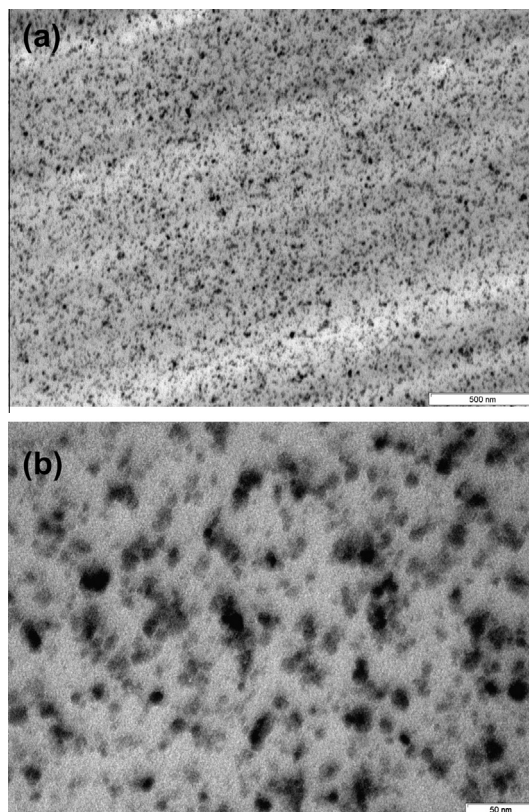
**Fig. 12.** Transmission optical microscopy (TOM) image of fractal aggregates at the air-polymer interface for the film containing 1 wt% NPs. Reproduced with permission from Gómez et al. [14].

shows the different steps of the self-assembly process and Fig. 12 shows a transmission optical microscopy (TOM) image of the interface of a film containing 1 wt% NPs [14]. The main difference in this morphology with respect to the one shown in Section 2.2 is the fact that the individual 2-nm NPs were still present in the large particles. Relatively high temperatures would have been needed to produce the growth by coalescence of the small gold NPs at the beginning of the phase separation process.

### 2.5. Limiting PIPS to a local scale

In many cases it is desired to keep the initial homogeneous dispersion of NPs in the final material or, at least, to limit aggregation of NPs to a local scale. This may be achieved by matching the chemical structures of the polymer and the ligands stabilizing the NPs, and by selecting reaction conditions providing a slow phase separation rate compared to the polymerization rate. The synthesis of remotely-activated shape memory polymers is an example where it is desired to limit PIPS to a local scale.

Shape memory polymers are advanced materials that can change their shapes by an external stimulus (thermal, magnetic, electrical, optical, etc.). They are used in space-deployable structures, smart textiles, artificial muscles and many other fields [15,16]. Due to their excellent thermomechanical properties, cross-linked epoxies are widely used as matrices for shape memory polymers [17–19]. Magnetic  $\text{Fe}_3\text{O}_4$  NPs dispersed in the epoxy matrix can be employed for the remote actuation of shape memory epoxies. When these nanocomposites are introduced into an alternating magnetic field, magnetization reversal processes (magnetic hyperthermia) produce release of heat and a temperature increase that activates the shape recovery. But the main question is how a



© American Chemical Society 2012

**Fig. 13.** TEM images of the nanocomposite containing 8 wt%  $\text{Fe}_3\text{O}_4$  NPs at two different magnifications (bars indicate 500 nm and 50 nm, respectively). Reproduced with permission from Puig et al. [21].

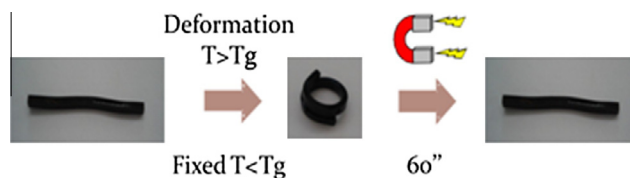


**Fig. 14.** A bar of the epoxy nanocomposite containing 8 wt% of  $\text{Fe}_3\text{O}_4$  NPs with a glass transition temperature ( $T_g$ ) equal to 58 °C (maximum of  $\tan \delta$ ), was deformed at 70 °C and cooled under loading to room temperature, fixing the shape. It was then placed in an alternating magnetic field for 60 s producing a temperature increase above  $T_g$  allowing complete recovery of the initial shape.

stable dispersion of  $\text{Fe}_3\text{O}_4$  NPs in epoxy precursors can be achieved. Obviously there is a need to make the chemical structure of the organic ligands used to stabilize the NPs compatible with the

structure of the epoxy precursors. Several conventional synthetic methods use oleic acid as a stabilizer of Fe<sub>3</sub>O<sub>4</sub> NPs [20]. How can these hydrophobic NPs be homogeneously dispersed in polar epoxy precursors? A possible answer is to modify the precursors using a hydrophobic component.

The reaction of a DGEBA excess with oleic acid (0.154 mole of carboxylic acid per mole of epoxy groups), catalyzed by a tertiary amine, led to a hydrophobic epoxy precursor that produced a homogeneous dispersion of 9.5 nm-Fe<sub>3</sub>O<sub>4</sub> NPs [21]. Subsequently to this reaction, homopolymerization of epoxy groups initiated by the same tertiary amine led to a polymer network. Fig. 13 shows TEM images of nanocomposites containing 8 wt% Fe<sub>3</sub>O<sub>4</sub> NPs at two different magnifications. The image with the lower magnification shows a homogeneous dispersion of clusters of NPs in the epoxy matrix. The image taken at a higher magnification shows the presence of individual NPs and clusters containing few NPs. Therefore, the hydrophobic modification of the epoxy precursor enabled to keep an excellent dispersion of NPs and limited phase separation to a local scale. Extensive phase separation was prevented by the viscosity increase followed by gelation.

A bar of the epoxy nanocomposite containing 8 wt% of Fe<sub>3</sub>O<sub>4</sub> NPs with a glass transition temperature ( $T_g$ ) equal to 58 °C (maximum of  $\tan \delta$ ), was deformed at 70 °C and cooled under loading to room temperature, fixing the shape. The bar was then placed in an alternating magnetic field for 60 s producing a temperature increase above  $T_g$  and allowing complete recovery of the initial shape (Fig. 14) [21].

## 2.6. Avoiding PIPS by covalently bonding the nanoparticles to the polymeric matrix

A convenient approach to keep the initial dispersion of NPs is to stabilize them with organic ligands bearing organic groups that can react with the precursors of the polymer. The reaction prevents phase separation of the NPs and produces (extra) cross-linking of the polymer matrix. This concept is extensively used to keep an initial good dispersion of carbon nanotubes along a polymerization [22], but it can also be employed for many other types of NPs. For example, POSS NPs (Fig. 1) with 8 organic moieties bearing reactive functionalities can act as co-monomers to generate epoxy networks without any evidence of phase separation [23–26]. Silver NPs with an average size equal to 4 nm were synthesized and stabilized with organic groups with the chemical structure shown in Fig. 15 [27]. These NPs were dispersed in DGEBA that was homopolymerized (3 h at 100 °C) by the addition of a tertiary amine [27]. NPs were covalently bonded to the epoxy network by chain transfer reactions to the OH groups present in the organic ligands. The incorporation of the silver NPs to the cross-linked structure was assessed by the constancy of the location of the plasmon band in UV-visible spectra and the fact that no leaching of silver NPs was observed after immersion of cross-linked samples in tetrahydrofuran for 3 months [27]. Fig. 16 shows the comparison of DSC thermograms of the neat epoxy matrix and a nanocomposite containing 0.33 wt% silver NPs [27]. The extra cross-linking produced

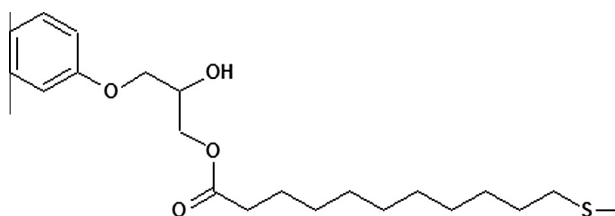


Fig. 15. Chemical structure of the organic group used as stabilizer of 4-nm silver NPs.

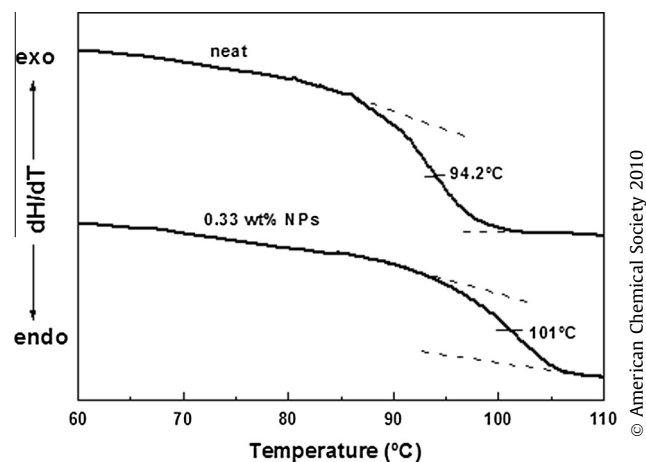


Fig. 16. DSC thermograms of the neat epoxy matrix and the nanocomposite containing 0.33 wt% NPs. Reproduced with permission from dell'Erba et al. [27].

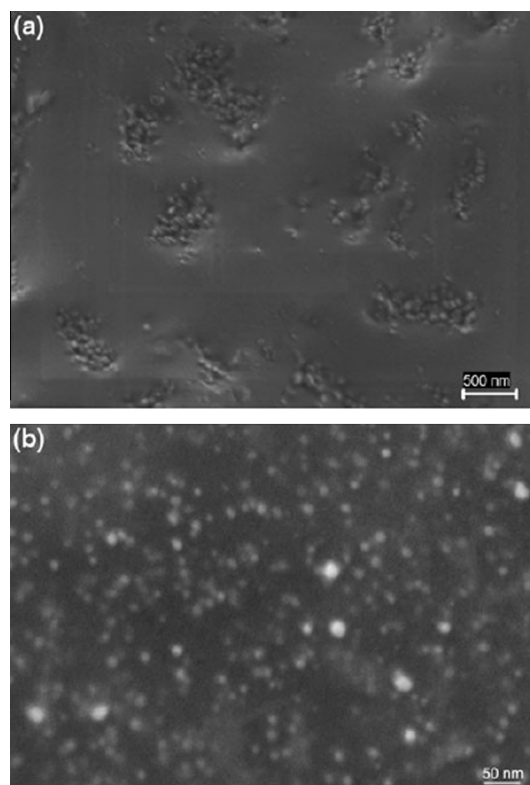
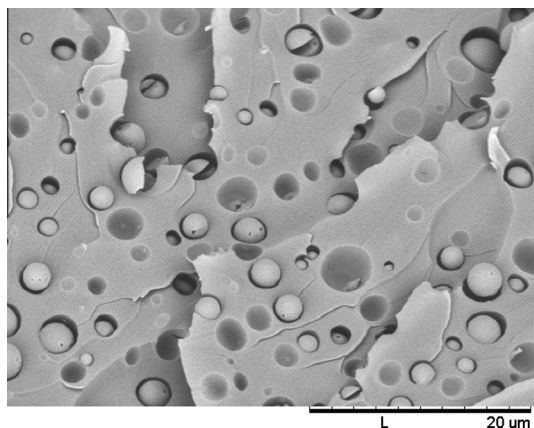


Fig. 17. Field-emission scanning electron microscopy (FESEM) images of the surface of a film composed of 1.5-nm gold NPs crosslinked by their organic ligands by a sol-gel reaction in solution, at two different magnifications; image (b) is a magnification of a smooth region of image (a). Reproduced with permission from dell'Erba et al. [29].

by the multifunctional silver NPs increased the glass transition temperature by about 7 °C.

An interesting case is the synthesis of nanocomposites by cross-linking the functional groups present in the stabilizing ligands without the addition of any other co-monomer. These materials have been designated as omni-composites because they are entirely (Lat. *Omnino*) composed of nanoparticles and their stabilizing ligands [28]. The concept has been proved using Eu<sup>+3</sup>-doped LaF<sub>3</sub> nanoparticles stabilized with ligands containing trifluorovinyl ether groups that can undergo a thermal cyclodimerization



**Fig. 18.** SEM micrograph of an epoxy matrix with a dispersion of spherical PS domains that include gold NPs in their interior. Reproduced with permission from Romeo et al. [32]. Copyright 2012 Elsevier.

reaction leading to a cross-linked network [28]. The nanocomposites were optically transparent and contained 78 wt% inorganic material. They exhibited a high-intensity emission due to the large loading of NPs and a low scattering because of the efficient dispersion of individual NPs.

The covalent bonding of NPs through their stabilizing ligands in the presence of a solvent, may lead to the formation of clusters of covalently bonded NPs in the course of polymerization. For example, 1.5-nm gold NPs functionalized with organic ligands bearing trialkoxysilane groups were dispersed in dimethylformamide and cross-linked by a sol–gel reaction, adding a formic acid solution [29]. Self-standing flexible films were obtained exhibiting a distribution of clusters of NPs (Fig. 17). Domains with a size in the range of 500 nm were originated by the agglomeration of 50-nm clusters (Fig. 17a). The inter-domain space is composed of 20-nm clusters interconnected by smaller clusters up to individual NPs (Fig. 17b). This morphology was generated by a nucleation-growth process of clusters of individual NPs cross-linked by their organic ligands, reaching sizes of about 50 nm. These clusters were self-assembled into 500-nm domains. But the whole structure was interconnected through covalent bonds leading to the self-standing film containing 77 wt% gold present in the core of 1.5-nm NPs.

### 3. PIPS in ternary NPs/modifier/reactive solvent formulations

#### 3.1. PIPS in ternary NPs/linear polymer/reactive solvent formulations

An initial homogeneous solution of a linear polymer (a rubber or a thermoplastic) in precursors of a thermosetting polymer leads

to a variety of morphologies by PIPS [1]. Depending on the initial composition, the resulting matrix may be formed by the cross-linked polymer or by the linear polymer. But in a range of intermediate compositions different morphologies may be obtained, such as co-continuous structures (both the linear and the cross-linked polymer form continuous phases) or double-phase morphologies where both dispersed domains of the linear polymer in the thermoset and dispersed domains of the cross-linked polymer in the linear polymer, are observed in different regions of the material [30,31]. These biphasic materials can be employed as templates for the self-assembly of NPs included as a third component in the initial formulation.

Gold NPs with an average size close to 2 nm and stabilized with dodecyl groups were incorporated (1 wt%) to a solution of polystyrene (PS, 10 wt%) in the precursors of a cross-linked epoxy [32]. During polymerization, PS and gold NPs were segregated from the epoxy phase leading to a black-colored and optically homogeneous material. SEM micrographs showed a dispersion of spherical PS domains with an average size close to 4 μm (Fig. 18). Gold NPs were located inside the PS domains as shown by TEM images (Fig. 19). Most of the NPs were segregated to a region close to the interface with the epoxy matrix. SAXS spectra revealed that NPs were self-organized in a body-centered cubic (bcc) crystalline structure [32].

This approach may be extended to different combinations of linear polymers and reactive solvents. In particular it could be interesting to select systems that develop co-continuous structures. In this case it might be possible to self-assemble NPs in an interface percolating throughout the material. Depending on the nature of the NPs core and the organic ligands, different properties (e.g., optical, electrical, mechanical) might be generated by the simple PIPS process.

#### 3.2. PIPS in ternary NPs/block copolymer (BCP)/reactive solvent formulations

Block copolymers (BCP) can self-assemble by PIPS during formation of a polymer network [33]. In this process, both blocks of the BCP are initially miscible with the precursors of the thermosetting polymer but one of the blocks phase separates in the course of polymerization while the other one remains miscible with the thermoset at least up to high conversions. This enables to self-assemble the BCP in the final material in a variety of phases that depend on the nature of the BCP, the initial composition and the cure cycle [34]. For example, a BCP composed of PS and polyethylene oxide (PEO) blocks can be dissolved in epoxy precursors at the polymerization temperature. PS blocks phase separate during polymerization but PEO blocks remain miscible with the cross-linked polymer. Depending on the size of both blocks and the initial concentration, different morphologies can be obtained.

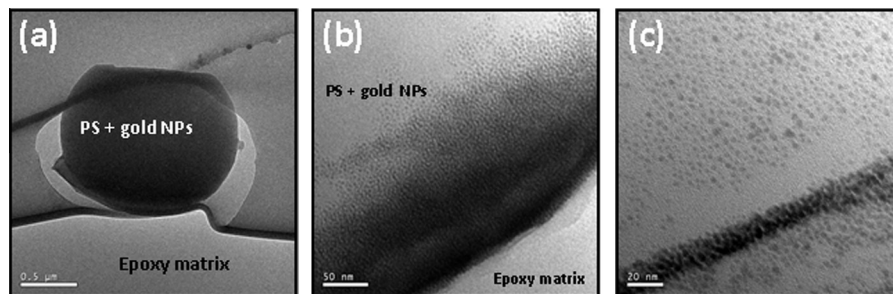


**Fig. 19.** TEM images of an epoxy matrix with a dispersion of spherical PS domains that include gold NPs in their interior. (a) Image showing the electronic contrast between PS domains and the epoxy matrix due to the presence of gold NPs inside PS domains, (b) and (c) are images obtained with a higher magnification. Reproduced with permission from Romeo et al. [32]. Copyright 2012 Elsevier.



**Fig. 20.** TEM image of the morphology obtained by PIPS of PS ( $M = 32,000$ )-b-PEO ( $M = 11,000$ ) dissolved in a 40 wt% concentration in epoxy precursors based on stoichiometric amounts of diglycidyl ether of bisphenol A (DGEBA) and 4,4'-methylenebis(2,6-diethylaniline) (MDEA).

As an example, Fig. 20 shows a TEM image of the morphology obtained by PIPS of PS ( $M = 32,000$ )-b-PEO ( $M = 11,000$ ) dissolved in a 40 wt% concentration in epoxy precursors based on stoichiometric amounts of diglycidyl ether of bisphenol A (DGEBA) and 4,4'-methylenebis(2,6-diethylaniline) (MDEA). The BCP self-assembled into a structure of hexagonally packed cylinders with PS cores and PEO/epoxy shells. This was also confirmed by SAXS spectra.

Block copolymers offer the possibility of controlling the NPs self-assembly and to develop different responses to external optical, magnetic or electrical fields [35,36]. The self-assembly of NPs can be produced by PIPS as discussed in the previous section. For example,  $\text{TiO}_2$  NPs were included into an epoxy/amine formulation together with a PS-b-PEO BCP [37,38].  $\text{TiO}_2$  NPs were confined in the PEO/epoxy regions close to the interface with PS domains. Fig. 21 shows AFM and TEM images of the morphology developed by PIPS in a formulation containing 20 wt% BCP and 20 wt% NPs [37]. The BCP self-assembled as hexagonally packed PS cylinders in a PEO/epoxy matrix.  $\text{TiO}_2$  dispersed in the PEO/epoxy domains appear as bright points in AFM images and dark points in the TEM image. The materials were transparent and exhibited high UV shielding efficiency, high visible light transparency as well as high water repellence [37,38].

#### 4. Future trends

The selected examples illustrate the variety of morphologies that may be generated by PIPS, starting from homogeneous

dispersions of NPs in reactive solvents. The interest in this field arises from the simplicity of the process: once the initial formulation and the polymerization process are defined, the desired distribution of NPs in the cured material is automatically generated. Future trends in this field can be associated with the development of practical applications that require a specific self-assembly pattern of NPs in a cross-linked polymer. For example, it would be of interest to adapt this process to self-assemble silver nanowires as a percolated structure inside a polymer film. The resulting material would exhibit transparency and high electrical conductivity and could be used in touch screen devices. Percolating structures of carbon nanotubes produced by PIPS could be also generated by this technique to increase the thermal or electrical conductivity of a nanocomposite. These percolated structures can be segregated to the surface during the process or, eventually, can be produced using an adequate template (e.g., a block copolymer).

The use of this technique to incorporate different types of NPs into a fiber-reinforced polymer is a completely open field. In this case, NPs could be segregated and self-assembled at the fiber interface modifying mechanical, thermal or electrical properties of the composite. Another field of increasing interest is related to the plasmon excitation of metallic NPs. The irradiation of the material with visible light with a wavelength in the region of the plasmon band of NPs, generates local temperature fields that may be used to initiate polymerization of the initial solution [39,40], or to produce chemical changes in the cross-linked network. As an example, thermally-activated transesterification reactions can be employed for the self-healing of cross-linked networks containing 2-hydroxyester chemical bonds [41–44]. The incorporation of silver or gold NPs into these networks could activate transesterification reactions by laser irradiation. Work is in progress in this direction.

#### 5. Conclusions

The use of polymerization-induced phase separation (PIPS) to produce the self-assembly of NPs in neat and modified polymers was reviewed through several selected examples. NPs can be homogeneously dispersed in the precursors of a polymer (reactive solvent) by an adequate selection of the organic ligands used as stabilizers. PIPS can be conveyed to generate a variety of morphologies such as crystalline platelets, self-assembled structures with a hierarchical order and partitioning at the interface, and bidimensional patterns of NPs at the film surface. But phase separation can be prevented or limited to a local scale when the polymerization rate is much higher than the phase separation rate or by covalently bonding the NPs to the polymer.

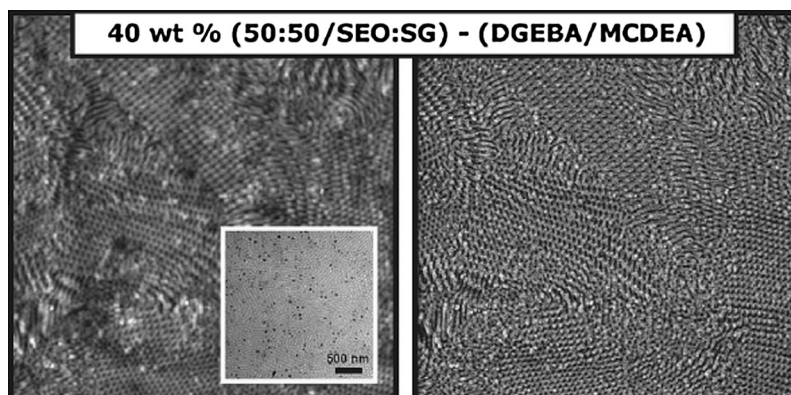


**Fig. 21.** AFM (left/right: height/phase) ( $5 \times 5 \mu\text{m}$ ) of morphologies generated in an epoxy formulation containing 20 wt% PS ( $M = 59,000$ )-b-PEO ( $M = 31,000$ ) and 20 wt%  $\text{TiO}_2$  NPs. The inset in the left is a TEM image of the same sample. Reproduced with permission from Gutierrez et al. [37]. Copyright 2011 Elsevier.

NPs can be also self-assembled by introducing templates such as linear polymers or block copolymers (BCP) in the initial formulation. In this case, PIPS produces the phase separation of a phase rich in the linear polymer or in one of the blocks of the BCP. Depending on the nature of the stabilizing ligands, NPs can be concentrated in one of the resulting phases or at the interfacial region. Blends of a linear polymer and thermoset precursors used in concentrations leading to co-continuous structures might be of interest to generate percolating paths of NPs' self-assemblies in the final material. This one-step process can be used to synthesize materials with a set of useful properties like electrical conductivity.

### Acknowledgments

The financial support of the National Research Council (CONICET), the National Agency for the Promotion of Science and Technology (ANPCyT), and the University of Mar del Plata, Argentina, is gratefully acknowledged.

### References

- [1] R.J.J. Williams, B.A. Rozenberg, J.P. Pascault, *Adv. Polym. Sci.* 128 (1997) 95–156.
- [2] E.R. Soulé, J. Borrajo, R.J.J. Williams, *Macromolecules* 40 (2007) 8082–8086.
- [3] C. Di Luca, E.R. Soulé, I.A. Zucchi, C.E. Hoppe, L.A. Fasce, R.J.J. Williams, *Macromolecules* 43 (2010) 9014–9021.
- [4] M. Brust, M. Walker, D. Bethell, D.J. Schiffrin, R. Whyman, *J. Chem. Soc., Chem. Commun.* (1994) 801–802.
- [5] I.A. Zucchi, C.E. Hoppe, M.J. Galante, R.J.J. Williams, M.A. López-Quintela, L. Matějka, M. Slouf, J. Pleštil, *Macromolecules* 41 (2008) 4895–4903.
- [6] M.M. Maye, W. Zheng, F.L. Leibowitz, N.K. Ly, C.J. Zhong, *Langmuir* 16 (2000) 490–497.
- [7] M.M. Maye, C.J. Zhong, *J. Mater. Chem.* 10 (2000) 1895–1901.
- [8] B.P. Binks, *Curr. Opin. Colloid Interface Sci.* 7 (2002) 21–41.
- [9] M.Y. Lin, H.M. Lindsay, D.A. Weitz, R.C. Ball, R. Klein, P. Meakin, *Nature* 339 (1989) 360–362.
- [10] T.A. Witten, L.M. Sander, *Phys. Rev. Lett.* 47 (1981) 1400–1403.
- [11] P. Meakin, *Phys. Rev. Lett.* 51 (1983) 1119–1122.
- [12] C. Paquet, E. Kumacheva, *Adv. Funct. Mater.* 17 (2007) 3105–3110.
- [13] J. Greener, T.H. van der Loop, C. Paquet, G. Scholes, E. Kumacheva, *Langmuir* 25 (2009) 3173–3177.
- [14] M.L. Gómez, C.E. Hoppe, I.A. Zucchi, R.J.J. Williams, M.I. Giannotti, M.A. López-Quintela, *Langmuir* 25 (2009) 1210–1217.
- [15] P.T. Mather, X. Luo, I.A. Rousseau, *Annu. Rev. Mater. Res.* 39 (2009) 445–471.
- [16] A. Lendlein, *J. Mater. Chem.* 20 (2010) 3332–3334.
- [17] T. Xie, I.A. Rousseau, *Polymer* 50 (2009) 1852–1856.
- [18] D.M. Feldkamp, I.A. Rousseau, *Macromol. Mater. Eng.* 295 (2010) 726–734.
- [19] A.B. Leonardi, L.A. Fasce, I.A. Zucchi, C.E. Hoppe, E.R. Soulé, C.J. Pérez, R.J.J. Williams, *Eur. Polym. J.* 47 (2011) 362–369.
- [20] J.K. Oha, J.M. Park, *Prog. Polym. Sci.* 36 (2011) 168–189.
- [21] J. Puig, C.E. Hoppe, L.A. Fasce, C.J. Pérez, Y. Piñero-Redondo, M. Bañobre-López, M.A. López-Quintela, J. Rivas, R.J.J. Williams, *J. Phys. Chem. C* 116 (2012) 13421–13428.
- [22] P.C. Ma, S.Y. Mo, B.Z. Tang, J.K. Kim, *Carbon* 48 (2010) 1824–1834.
- [23] J. Choi, J. Harcup, A.F. Yee, Q. Zhu, R.M. Laine, *J. Am. Chem. Soc.* 123 (2001) 11420–11430.
- [24] J. Choi, A.F. Yee, R.M. Laine, *Macromolecules* 36 (2003) 5666–5682.
- [25] Y. Ni, S. Zheng, K. Nie, *Polymer* 45 (2004) 5557–5568.
- [26] Y.L. Liu, G.P. Chang, K.Y. Hsu, F.C. Chang, *J. Polym. Sci., A. Polym. Chem.* 44 (2006) 3825–3835.
- [27] I.E. dell'Erba, C.E. Hoppe, R.J.J. Williams, *Langmuir* 26 (2010) 2042–2049.
- [28] J.R. DiMaio, B. Kokuoz, J. Ballato, *J. Am. Chem. Soc.* 130 (2008) 5628–5629.
- [29] I.E. dell'Erba, C.E. Hoppe, R.J.J. Williams, *J. Nanopart. Res.* 14 (2012). article 1098.
- [30] J.P. Pascault, R.J.J. Williams, in: D.R. Paul, C.B. Bucknall (Eds.), *Polymer Blends, Volume 1: Formulation*, Wiley, New York, 2000, pp. 379–415.
- [31] M. Rico, J. López, B. Montero, R. Bellas, *Eur. Polym. J.* 48 (2012) 1660–1673.
- [32] H.E. Romeo, A. Vílchez, J. Esquena, C.E. Hoppe, R.J.J. Williams, *Eur. Polym. J.* 48 (2012) 1101–1109.
- [33] S. Zheng, in: J.P. Pascault, R.J.J. Williams (Eds.), *Epoxy Polymers: New Materials and Innovations*, Wiley-VCH, Weinheim, 2010, pp. 81–108.
- [34] H.E. Romeo, I.A. Zucchi, M. Rico, C.E. Hoppe, R.J.J. Williams, *Macromolecules* 46 (2013) 4854–4861.
- [35] R.V. Thompson, V.V. Ginzburg, M.W. Matsen, A.C. Balazs, *Science* 292 (2001) 2469–2472.
- [36] J.J. Chiu, B.J. Kim, E.J. Kramer, D.J. Pine, *J. Am. Chem. Soc.* 127 (2005) 5036–5037.
- [37] J. Gutierrez, I. Mondragon, A. Tercjak, *Polymer* 52 (2011) 5699–5707.
- [38] A. Tercjak, J. Gutierrez, M.D. Martin, I. Mondragon, *Eur. Polym. J.* 48 (2012) 16–25.
- [39] C. Fasciani, C.J. Bueno, *Org. Lett.* 13 (2011) 204–207.
- [40] K.G. Stamplecoskie, N.L. Pacioni, D. Larson, J.C. Scaiano, *J. Am. Chem. Soc.* 133 (2011) 9160–9163.
- [41] D. Montarnal, M. Capelot, F. Tournilhac, *Science* 334 (2011) 965–968.
- [42] M. Capelot, D. Montarnal, F. Tournilhac, L. Leibler, *J. Am. Chem. Soc.* 134 (2012) 7664–7667.
- [43] M. Capelot, M.M. Unterlass, F. Tournilhac, L. Leibler, *ACS Macro Lett.* 1 (2012) 789–792.
- [44] F.I. Altuna, V. Pettarin, R.J.J. Williams, *Green Chem.* 15 (2013) 3360–3366.